

Recovering True Metal Abundances of the ICM

Silvia Pellegrini

*Astronomy Department, Bologna University, via Ranzani 1, I-40127
 Bologna*

Luca Ciotti

*Bologna Astronomical Observatory, via Ranzani 1, I-40127 Bologna
 Princeton University Observatory, 08544 Princeton, NJ, USA*

Abstract. Recovering the true *average* abundance of the intracluster medium (ICM) is crucial for estimates of its global metal content, which in turn is linked to its past evolution and to the star formation history of the stellar component of the cluster. We analyze here how abundance gradients affect commonly adopted estimates of the average abundance, assuming various plausible ICM density and temperature profiles. We find that, adopting the observed abundance gradients, the true average mass weighted abundance is less than (although not largely deviating from) the commonly used emission weighted abundance.

1. Introduction

The metal content of the ICM has proved to be a powerful tool to constrain the past supernova history of the stellar population of galaxy clusters, being it directly linked to the total number of supernovae exploded in the cluster (e.g., Renzini et al. 1993). Supernovae also provide a heating mechanism of the ICM, via galactic winds that they power, and the relevance of this heating is a much debated topic in recent studies of ICM evolution (e.g., Ponman, Cannon, & Navarro 1999; Wu, Fabian, & Nulsen 2000; Lloyd-Davies, Ponman, & Cannon 2000). So, estimates of the mass of metals in the ICM (M_{ICM}^Z) are precious pieces of information, and the more accurate they are, the more constraining they can be in recovering the past supernova activity and from here the past histories of star formation and heating and evolution of the ICM. A quantity strictly related to M_{ICM}^Z is the *average abundance* $\langle Z_{\text{ICM}} \rangle \equiv M_{\text{ICM}}^Z / M_{\text{ICM}}$. There are two main possibilities to estimate $\langle Z_{\text{ICM}} \rangle$. One is given by:

$$\boxed{1} \quad \langle Z_{\text{ICM}} \rangle_{\text{depr}} = \frac{\int \rho_{\text{ICM}}(\mathbf{x}) Z_{\text{ICM}}(\mathbf{x}) d^3 \mathbf{x}}{\int \rho_{\text{ICM}}(\mathbf{x}) d^3 \mathbf{x}},$$

where $\rho_{\text{ICM}}(\mathbf{x})$ and $Z_{\text{ICM}}(\mathbf{x})$ are three-dimensional gas density and abundance distributions (e.g., derived from deprojection of observed two-dimensional quan-

tities). The other is an *emission weighted* average abundance:

$$\boxed{2} \quad \langle Z_{\text{ICM}} \rangle_L = \frac{\int n_{\text{ICM}}^2(\mathbf{x}) \Lambda[T(\mathbf{x}), Z(\mathbf{x})] Z_{\text{ICM}}(\mathbf{x}) d^3 \mathbf{x}}{\int n_{\text{ICM}}^2(\mathbf{x}) \Lambda[T(\mathbf{x}), Z(\mathbf{x})] d^3 \mathbf{x}},$$

where Λ is the cooling function. This $\langle Z_{\text{ICM}} \rangle_L$ is estimated for example as a fit parameter when modeling the observed X-ray spectrum of the whole ICM.

2. The problem

There are a few serious problems with estimating $\langle Z_{\text{ICM}} \rangle$ using method $\boxed{1}$. In fact, for many/most clusters we do not know:

- the *shape* of the ICM distribution;
- the *viewing angles* under which we are observing the ICM distribution.

So, we cannot unambiguously deproject the observed quantities to derive 3-D ones such as $Z_{\text{ICM}}(\mathbf{x})$, $\rho_{\text{ICM}}(\mathbf{x})$ and $T_{\text{ICM}}(\mathbf{x})$. In addition, it is well known that deprojection is a very demanding process, sensitive also to:

- the properties of the *instrumental PSF*;
- the *measurement errors* (e.g., Finoguenov & Ponman 1999).

Correspondingly, there are clear advantages with method $\boxed{2}$:

- the knowledge of the true shape of the ICM distribution is not required and the result is *independent of* the viewing angles;
- it does *not suffer from* instrumental effects and amplification of measurement errors.

- the average $\langle Z_{\text{ICM}} \rangle_L$ is the *only accessible information* that we may have for distant clusters or those for which there are not counts enough for a spatially resolved spectroscopy (many more of these are likely to be observed/discovered soon, thanks to *Chandra* and *XMM*).

Unfortunately, method $\boxed{2}$ has one problem, whose relevance has not been investigated so far. *Emission weighted* average abundances $\langle Z_{\text{ICM}} \rangle_L$ derived from observed X-ray spectra are equal to the *true* $\langle Z_{\text{ICM}} \rangle$ only in case of a spatially independent metal distribution. So, only if $Z(\mathbf{x}) = Z_0$ constant, then $\langle Z_{\text{ICM}} \rangle_L = \langle Z_{\text{ICM}} \rangle = Z_0$. Recently *spatial abundance gradients* have been derived for the ICM of many clusters from *ASCA* and *BeppoSAX* data (e.g., Finoguenov, David, & Ponman 2000; Irwin & Bregman 2001; De Grandi & Molendi 2001). When such gradients are present, in general $\langle Z_{\text{ICM}} \rangle_L \neq \langle Z_{\text{ICM}} \rangle$, in a way dependent on the spatial distribution of ρ_{ICM} , T_{ICM} , Z_{ICM} . Here we address the following point: how much discrepant are $\langle Z_{\text{ICM}} \rangle_L$ and $\langle Z_{\text{ICM}} \rangle$?

Our approach to find the answer is to “calibrate” the $\langle Z_{\text{ICM}} \rangle_L / \langle Z_{\text{ICM}} \rangle$ ratio using **many** plausible (spherically symmetric) profiles for ρ_{ICM} , T_{ICM} and Z_{ICM} . The ingredients entering the estimates of $\langle Z_{\text{ICM}} \rangle_L$ and $\langle Z_{\text{ICM}} \rangle$ are the following:

- 1) the cooling function $\Lambda = \Lambda(T, Z)$ over (0.5–10) keV; this has been calculated with the thermal X-ray emission code of J. Raymond (that gives the same results as the MEKAL model within XSPEC for $kT \geq 3$ keV).

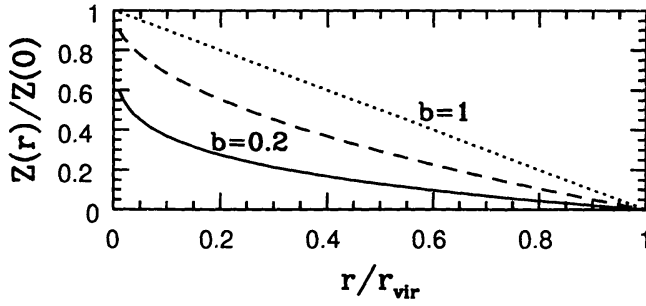


Figure 1. Abundance profiles adopted in this work

- 2) An abundance profile described by $Z_{\text{ICM}}(r) = Z_0 \times [1 - (r/r_{\text{vir}})^b]$, where b is a free parameter (Fig. 1) and r_{vir} is the cluster virial radius.
- 3) Various ρ_{ICM} and T_{ICM} profiles (Figs. 2 and 3). In a *first set* of models we assume the ICM to be in (non self-gravitating) hydrostatic equilibrium within a chosen cluster (dark matter) potential well, both in the isothermal and polytropic case. In a *second set* of models we consider a cooling flow description.

3. Models of ICM in hydrostatic equilibrium

3.1. Description

In this first set of ICM models we explored:

a. The “NFW” cluster potential well (Navarro, Frenk, & White 1996), where the density profile of the gravitating matter is of the form $\rho_{\text{cl}}(r) = 4\rho_{\text{cl}}(r_s)r_s^3/r(r+r_s)^2$. The *isothermal* and *polytropic* ICM density profiles are given by:

$$\rho_{\text{ICM}}^{\text{is}}(r) = \rho_0 \times \exp\left[\frac{\mu m_p}{kT_0}(\phi_0 - \phi)\right], \quad \rho_{\text{ICM}}^{\text{pol}}(r) = \rho_0 \times \left[1 + \frac{\gamma - 1}{\gamma} \frac{\mu m_p}{kT_0}(\phi_0 - \phi)\right]^{\frac{1}{\gamma-1}}.$$

In the polytropic cases the temperature profile is obviously given by

$$T_{\text{ICM}}^{\text{pol}}(r) = T_0 \times \left[\frac{\rho_{\text{ICM}}(r)}{\rho_0}\right]^{\gamma-1}.$$

b. The power law models, in which the cluster density profile is given by $\rho_{\text{cl}}(r) = \rho_n \times (r/r_n)^{-\alpha}$, with $\alpha < 2$. We have now

$$\rho_{\text{ICM}}^{\text{is}}(r) = \rho_0 \times \exp\left(-\frac{\mu m_p}{kT_0}\phi\right), \quad \rho_{\text{ICM}}^{\text{pol}}(r) = \rho_0 \times \left[1 - \left(\frac{r}{r_{\text{vir}}}\right)^{2-\alpha}\right]^{\frac{1}{\gamma-1}}.$$

c. The “standard” β -models (e.g., Cavaliere & Fusco Femiano 1976), where the surface brightness profile of the hot ICM is described by $\Sigma_X(R) = \Sigma_{X0} \times [1 + (R/R_c)^2]^{0.5-3\beta}$, and $\beta = 0.5 - 0.8$ (Mohr et al. 1999, Jones & Forman

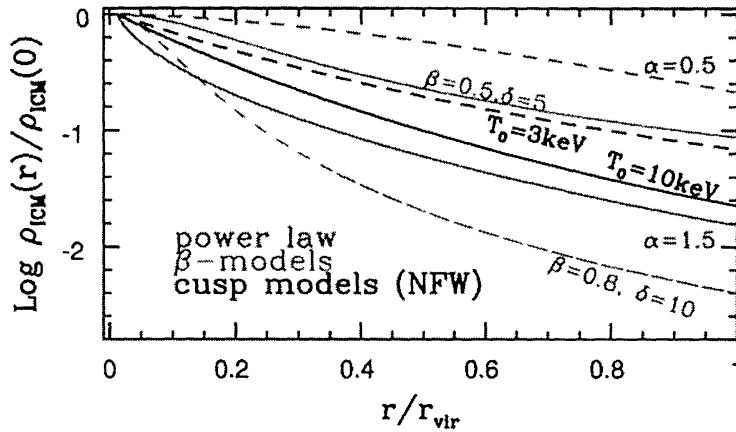


Figure 2. The density profiles of hydrostatic equilibrium models described in section 3, in the isothermal case.

1999). The (untruncated) ICM density profiles are given by:

$$\rho_{\text{ICM}}^{\text{is}}(r) = \rho_0 \times \left[1 + \left(\frac{r}{R_c} \right)^2 \right]^{-3\beta/2}, \quad \rho_{\text{ICM}}^{\text{pol}}(r) = \rho_0 \times \left[1 + \left(\frac{r}{R_c} \right)^2 \right]^{f(\beta, \gamma)},$$

where $f(\beta, \gamma)$ can be found in Ettori (2000). Both density distributions are then truncated at a radius $R_t = \delta R_c$, with δ a free parameter.

Constraints on the parameter values have been derived from observational results and from the relations $M_{200} - \langle T_X \rangle$ (Navarro et al. 1996), $\langle T_X \rangle - r_{200}$ (Evrard et al. 1996) and $\sigma^2 - \langle T_X \rangle$ (Xue & Wu 2000).

3.2. Results

We estimated $\langle Z_{\text{ICM}} \rangle_L / \langle Z_{\text{ICM}} \rangle$ by adopting the following parameter values:

1) for the abundance profile $b = 0.2$, i.e., we considered a sort of ‘‘cuspy’’ profile, as observed in some clusters (e.g., De Grandi & Molendi 2001; Arnaud, this meeting), and $b = 1$, a linear dependence on radius. The results are almost independent of Z_0 .

2) the temperatures are $T_0 = 3$ and 10 keV in the isothermal case; these are central temperatures, in the polytropic case. This assumption encompasses the values observed for rich galaxy clusters (e.g., Markevitch et al. 1998).

3) $1 < \gamma \leq 5/3$ in the polytropic case. This includes the $\gamma = 1.2$ value that gives a ‘‘good’’ fit of some observed temperature profiles for ICM’s described by a β -model (Markevitch et al. 1998).

4) for the power law models $\alpha = 0.5$ and 1.5.

5) for the β -models: $\beta = 0.5$ and 0.8, $\delta = 5$ and 10.

The general trend of the values derived for $\langle Z_{\text{ICM}} \rangle_L / \langle Z_{\text{ICM}} \rangle$ is that:

- $\langle Z_{\text{ICM}} \rangle_L / \langle Z_{\text{ICM}} \rangle$ always increases for centrally steeper abundance profiles (i.e., lower b values) and steeper gas density profiles (i.e., higher T_0 , α , β and δ).

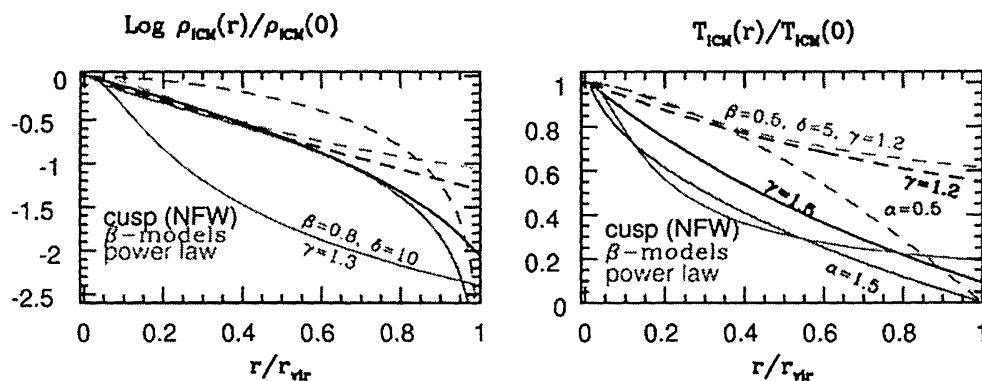


Figure 3. The density and temperature profiles of hydrostatic equilibrium models described in section 3, in the polytropic case.

- $\langle Z_{\text{ICM}} \rangle_L / \langle Z_{\text{ICM}} \rangle$ is always > 1 , and it assumes the values below:

	isothermal case	polytropic case
a. NFW:	1.4–1.7	1.4–1.7
b. POWER LAW:	1.3–1.8	1.3–1.5
c. β -MODELS:	1.4–2.1	1.5–2.2
- The typical range of values for $\langle Z_{\text{ICM}} \rangle_L / \langle Z_{\text{ICM}} \rangle$ is 1.4–2, quite insensitive to variations of density and temperature profiles in the chosen (large) range.

4. Cooling flow models

We assume the ICM to be described by two gas phases, at two fixed temperatures T_{cool} and T_{amb} , in pressure equilibrium within the cooling radius r_{cool} . Outside r_{cool} there is only the ambient gas at T_{amb} (Ettori 2001). So:

$$\rho_{\text{ICM}}(r) = \rho_{0,\text{cool}} \times \left[1 - \left(\frac{r}{r_{\text{cool}}} \right)^2 \right]^{1.5\beta_{\text{cool}}} + \rho_{0,\text{amb}} \times \left[1 + \left(\frac{r}{r_c} \right)^2 \right]^{-1.5\beta_{\text{amb}}}.$$

Correspondingly the X-ray surface brightness profile is given by the superposition

$$\Sigma_X(R) = \Sigma_{X0,\text{cool}} \times \left[1 - \left(\frac{R}{r_{\text{cool}}} \right)^2 \right]^{0.5+3\beta_{\text{cool}}} + \Sigma_{X0,\text{amb}} \times \left[1 + \left(\frac{R}{r_c} \right)^2 \right]^{0.5-3\beta_{\text{amb}}}.$$

For two well studied cooling flow clusters, for which this decomposition has been made (Ettori 2001), we find $\langle Z_{\text{ICM}} \rangle_L / \langle Z_{\text{ICM}} \rangle$ as given in Table 1 (for $b = 0.2$ and 1).

5. Future developments

We plan to do the following further investigation:

Table 1. Results for cooling flow models

Cluster	δ	$r_c = r_{\text{cool}}$ (h_{50}^{-1} Mpc)	T_{cool} (keV)	T_{amb} (keV)	β_{cool}	β_{amb}	$\frac{\langle Z_{\text{ICM}} \rangle_L}{\langle Z_{\text{ICM}} \rangle}$
A1795	5.8	0.26	0.5–1.1	7.4	1.801	0.761	1.6–2.0
A2199	11.5	0.13	0.4–0.8	4.6	1.635	0.644	1.7–2.1

1) Calibrate $\langle Z_{\text{ICM}} \rangle_L / \langle Z_{\text{ICM}} \rangle$ for axisymmetric and triaxial models (not significantly different results are expected).

2) Calibrate $\langle Z_{\text{ICM}} \rangle_{\text{depr}} / \langle Z_{\text{ICM}} \rangle$ for axisymmetric and triaxial models, by considering their projection at different viewing angles, by circularizing and de-projecting their X-ray properties, by deriving putative 3-D $\rho_{\text{ICM}}(r)$ and $Z_{\text{ICM}}(r)$ and comparing $M_{\text{ICM,depr}}^Z = 4\pi \int r^2 \rho_{\text{ICM}}(r) Z_{\text{ICM}}(r) dr$ with the true value M_{ICM}^Z .

3) Evaluate $\langle Z_{\text{ICM}} \rangle_L / \langle Z_{\text{ICM}} \rangle$ for ICM's resulting from high resolution numerical hydrodynamic simulations that include dark matter, gas and star formation (Cen & Ostriker 2000).

References

- Cavaliere, A., & Fusco-Femiano, R. 1976, A&A, 49, 137
Cen, R., & Ostriker, J.P. 2000, ApJ, 538, 83
De Grandi, S., & Molendi, S. 2001, ApJ, 551, 153
Ettori, S. 2000, MNRAS, 318, 1041
Ettori, S. 2001, astro-ph/0005224
Evrard, A.E., Metzler, C.A., & Navarro, J.F. 1996, ApJ, 469, 494
Finoguenov, A., & Ponman, T.J. 1999, MNRAS, 305, 325
Finoguenov, A., David, L.P., & Ponman, T.J. 2000, ApJ, 544, 188
Irwin, J.A., & Bregman, J.N. 2001, ApJ, 546, 150
Jones, C., & Forman, W. 1999, ApJ, 511, 65
Lloyd-Davies, E.J., Ponman, T.J., & Cannon, D.B. 2000, MNRAS, 315, 689
Markevitch, M., Forman, W.R., Sarazin, C.L., & Vikhlinin, A. 1998, ApJ, 503, 77
Mohr, J.J., Mathiesen, B., & Evrard, E. 1999, ApJ517, 627
Navarro, J.F., Frenk, C.S., & White, S.D.M. 1996, ApJ, 462, 563
Ponman, T.J., Cannon, D.B., & Navarro, J.F. 1999, Nature, 397, 135
Renzini, A., Ciotti, L., D'Ercole, A., & Pellegrini, S. 1993, ApJ, 419, 52
Wu, K.K.S., Fabian, A.C., & Nulsen, P.E.J. 2000, MNRAS, 318, 889
Xue, Y., & Wu, X. 2000, ApJ, 538, 65